COVER PAGE

TITLE:

Current Status of Large Helical Device and Its Prospect for Deuterium Experiment

Authors:

M. Osakabe[1,2], Y. Takeiri[1,2], T. Morisaki[1,2], G. Motojima[1], K. Ogawa[1,2], M. Isobe[1,2], M. Tanaka[1], S. Murakami[3], A. Shimizu[1], K. Nagaoka[1], H. Takahashi[1], K. Nagasaki[4], H. Takahashi[1],T. Fujita[5], Y. Oya[6], M. Sakamoto[7], Y. Ueda[8], T. Akiyama[1], H. Kasahara[1], S. Sakakibara[1,2], R. Sakamoto[1,2] , M. Tokitani[1], H. Yamada[1,2], M. Yokoyama[1,2], Y. Yoshimura[1], and the LHD Experiment Group

Affiliations:

[1]*National Institute for Fusion Science, Natural Institutes of Natural Sciences, 322-6 Oroshi-cho, Toki 509-5292, Japan*
[2] *SOKENDAI (The Graduate University for Advanced Studies), 322-6 Oroshi-cho, Toki 509-5292, Japan*
[3]*Department of Mechanical Engineering and Science, Kyoto University, Kyoto 615-8540, Japan*
[4]*Institute of Advanced Energy, Kyoto University, Gokasho, Uji, Kyoto 611-0011, Japan*
[5]*Department of Energy Engineering and Science, Graduate School of Engineering, Nagoya University, Furo-cho, Chikusa-ku, Nagoya 464-8093, Japan*
[6]*Radioscience Research Laboratory, Faculty of Science, Shizuoka University, 836, Ohya, Suruga-ku, Shizuoka 422-8529, Japan*
[7]*Plasma Research Center, University of Tsukuba, Tsukuba, Ibaraki 305-8577, Japan*
[8]*Graduate School of Engineering, Osaka University, 2-1 Yamadaoka, Suita, Osaka 565-0871, Japan*

Responsible Author: Masaki Osakabe

Responsible Author's Mailing Address: 322-6 Oroshi, Toki, Gifu 509-5292, Japan

E-mail Address: osakabe.masaki@LHD.nifs.ac.jp

FAX number: +81-572-58-2634

Abstract ID number: 18945

Total number of pages: 25 (including this cover sheet)

Total number of tables: 2

Total number of figures:9

TITLE:

Current Status of Large Helical Device and Its Prospect for Deuterium Experiment

Authors:

M. Osakabe, Y. Takeiri, T. Morisaki, G. Motojima, K. Ogawa, M. Isobe, M. Tanaka, S. Murakami, A. Shimizu, K. Nagaoka, H. Takahashi, K. Nagasaki, T. Fujita, Y. Oya, M. Sakamoto, Y. Ueda, T. Akiyama, H. Kasahara, S. Sakakibara, R. Sakamoto, M. Tokitani, H. Yamada, M. Yokoyama, Y. Yoshimura and LHD experiment group

Abstract

Achievement of reactor relevant plasma condition in Helical type magnetic devices and exploration in its related plasma physics and fusion engineering are the aim of the Large Helical Device (LHD) project. In the recent experiments on LHD, we have achieved ion-temperature of 8.1keV at $1x10^{19}m^{-3}$ by the optimization of wall conditioning using long pulse discharge by Ion Cyclotron Heating (ICH). The electron temperature of 10keV at $1.6x10^{19}m^{-3}$ was also achieved by the optimization of Electron Cyclotron Heating (ECH). For further improvement in plasma performance, the upgrade of the Large Helical Device (LHD), including the deuterium experiment, is planned. In this paper, the recent achievements on LHD and the upgrade of LHD are described.

Keywords: LHD, deuterium experiment, high temperature operation, steady state operation, closed divertor

1. Introduction

Achievement of high-performance plasma close to self-sustained fusion plasma condition is one of the important issues in realizing a fusion reactor. The aim of the Large Helical Device (LHD) project is to realize the high performance plasmas relevant to the fusion plasma condition in a helical-type magnetic configuration and to explore the related plasma physics and fusion engineering. The following are major goals of the LHD project: achievement of (1) high temperature plasmas exceeding 10keV at electron density of $2x10^{19}m^{-3}$; (2) high density plasmas exceeding $4x10^{20}m^{-3}$ with electron temperature of 1.3keV; (3) high beta plasmas exceeding 5% at 1T; and (4) long pulse plasma operation exceeding 1 hour with 3MW input heating power. In the recent experiments on LHD, we have achieved ion-temperature of 8.1keV at $1x10^{19}m^{-3}$ by the optimization of wall conditioning using long pulse discharge by Ion Cyclotron Heating (ICH). The electron temperature of 10keV at $1.6x10^{19}m^{-3}$ was also achieved by the optimization of Electron Cyclotron Heating (ECH).

For further improvement in plasma performance, the deuterium experiment project is planned, and will start on the LHD from March 2017. The objectives of the experiment are:

(1) to realize high-performance plasmas in helical systems by confinement improvement and by upgraded facilities;

(2) to study the isotope effects on plasma confinement in toroidal plasma devices;

(3) to demonstrate the confinement capability of Energetic Particles (EPs) in helical systems; and

(4) to extend the research on the plasma-material interactions with long time scale using the benefits of the LHD's steady state operation ability.

In this paper, the recent results of LHD are shown and reviewed in section 2. Several devices are now in the process of being upgraded in preparation for the deuterium

experiments. The plan for the deuterium experiments and the upgrade of devices are shown in section 3. Some important topics in the deuterium experiment, including isotope effects, energetic particle physics and others, are discussed in section 4. Section 5 provides the summary.

2. Recent achievements of LHD

The LHD is a helical type magnetically confined device based on the heliotron configuration and is one of the world largest devices using super conducting magnets.[1] Confining magnetic fields are created by one pair of helical coils and by three pairs of planner coils. The typical plasma major radius, minor radius and plasma volume are 3.6m, 0.6m and 30m^3, respectively. The operational magnetic field strengths at the magnetic axis range between 0.42T and 3T. Most of the vacuum vessel (VV) of the LHD is covered by stainless steel protection plates with cupper back plates. The carbon plates are used for the place where the heat load onto the wall is significant, such as the counter wall of the ports for Neutral Beam Injectors (NBIs) (Ref. 2) and the target plates of the divertor.[3]

As main heating devices, the LHD has three tangential-NBIs (tNBIs) based on negative-ion sources and two radial-NBIs (rNBIs) based on positive-ion sources as shown in Fig. 1. (Ref. 4) The nominal injection energies of tNBI and rNBI are 180keV and 40keV for hydrogen atom injection, respectively. Total maximum injection powers reach 16MW for tNBIs and 12MW for rNBIs. The LHD also has ECH with three 77GHz gyrotrons and two 154GHz gyrotrons. Total injection power of ECH is 5MW for short pulse operation and 0.6MW for steady state operation.[5] The ICH is used as a main heating source for steady state operation. The typical operational frequency is 38.47MHz and the typical operation scenario is hydrogen minority heating in helium majority plasmas. The total injection power of ICH is about 6MW. (Ref.6)

The experiment was started in 1998 on LHD. Table I summarizes the target plasma parameters of LHD and its achievements. Recently, extension in high temperature region is mostly focused on LHD in order to demonstrate the ability to achieve reactor relevant high temperature plasmas and to clarify the physics which may arise in these plasmas. Figure 2(a) shows the typical ion temperature profile, electron temperature profile, and electron density profile at the high ion-temperature discharge on LHD where central ion temperature of 8.1keV at $1x10^{19}m^{-3}$ was achieved.[7, 8] As shown in the figure, an internal transport barrier with steep ion temperature gradient is formed in the region between r_{eff}=0.2 and 0.4m in this discharge. It was found that the "impurity hole," where most of the impurity ions were expelled from the core region of plasmas, was formed in the high ion temperature plasmas on LHD.[9, 10] The high electron temperature plasmas were also realized on LHD with the intensive electron heating by ECH (~5MW) at the center of the plasmas. Fig. 2(b) shows the typical electron temperature and density profiles. In the discharge, electron temperature exceeding 10keV was achieved at the electron density of $1.6\ x10^{19}m^{-3}$ and the Core Electron-Root Confinement (CERC[Ref.11]) was realized with the strongly focused ECH at the center of the plasmas.[12]

The steady state operation is another important topic in the recent LHD experiment. On LHD, a long pulse discharge with the electron density of $1x10^{19}m^{-3}$ and with the electron temperature of 2keV was successfully sustained up to 47 minutes by the combined heating with ICH (1MW) and ECH (0.2MW). Figure 3 shows waveforms of the long pulse discharge. The line averaged electron density was successfully maintained at $\sim1x10^{19}m^{-3}$ by the feedback control of the gas-puff fueling system in the discharge. In Fig. 3(c), the amount of particles fueled by the gas-puff system and that exhausted by the external vacuum pumps are shown by black and green curves, respectively. Since the heating scenario of ICH is hydrogen minority heating in helium majority plasma in the discharge, the helium was fueled

by the gas-puff. The slopes of these two curves correspond to the fueling rate by the gas-puff and pumping rate by the pumps, respectively. In Fig. 3(c), the orange curve corresponds to the difference of the two curves and indicates the amount of the particles exhausted by the first wall of the LHD-VV. The discharge can be divided into three time phases from the slope of the particle exhaust curve by the wall. At the initial phase of the discharge (t=0~250s), the wall retention was very large, i.e., the pumping speed by the wall (~0.4Pam^3/s) is much faster than that by the pumps (~0.03Pam^3/s). At the middle phase (t=250~1500s), the pumping speed by the wall becomes negative value, i.e., the slope of the curve becomes negative. This indicates the saturation of the wall and the emission of particles from the wall. This seems very natural since the total amount of particles captured by a material is finite and the captured particle might be released from the material when the temperature of the material increases due to the heat loads from the plasmas. What is surprising is that the recovery of particle pumping by the wall was observed at the final phase (t=1500s~). The mechanism of the recovery is not yet perfectly understood, but it is thought that the mixed-material layers, which are mainly composed of carbon and iron, deposited on the wall during the plasma discharge play an important role in the recovery.[13] By the long pulse discharge on LHD, a new phenomenon of the particle-material interaction, i.e., the recovery of the wall pumping, was found. This new finding is a benefit of the stable steady state operational ability of the LHD.

3. Upgrade of LHD for high performance operation and deuterium experiment on LHD

Upgrade of LHD is planned to extend the performance of LHD. The deuterium experiment is a part of this upgrade plan because the confinement improvement is expected by the isotope effect and because the increase of the injection power of positive-ion based

NBI (P-NBI) is expected by the use of deuterium ion beam with the increase of its injection energy.

The long-term schedule of deuterium experiments is shown in Table II. The deuterium experiment will start from March 2017 and is planned to proceed for nine years. With the amount of annual neutron yield, the deuterium experiment is divided into two periods. In the first six years, the annual neutron yield is limited to 2.1×10^{19}. On the other hand, the annual neutron yield will be increased to 3.2×10^{19} in the later three years. The first year of the deuterium experiment will be mainly dedicated to the commissioning of LHD for radiation safety, including the absolute calibration of neutron diagnostics. Retention studies on hydrogen isotopes in the vacuum vessel will also be a major task of the first year. From the second year through the sixth year of the deuterium experiment, we will undertake the improvement of the LHD plasma parameters, especially to extend the high ion temperature region of LHD plasmas, with deuterium discharges and with upgraded heating devices. Exploration in plasma physics using the benefit of deuterium experiment is another important task during this period, e.g., investigation of the isotope effect in helical plasmas, the confinement studies of energetic ions, the studies of Plasma-Material Interactions (PMIs), and other issues. The last three years will be used for integrated high-performance operations on LHD and development for the steady state operation scenarios.

In addition to the deuterium experiment, upgrades of several devices are also planned, and have been performed for improving the LHD performance. The upgrade of positive-ion based NBI is the one of them. Because the neutralization efficiency falls drastically as the energy of the beam increases above 40keV/amu in the case of positive-ion based NBI,[Ref.14] it is very difficult for positive-ion based NBI to increase the injection power by increasing its energy if the mass of the beam remains same. By changing the beam ion species from hydrogen to deuterium, the beam injection energy can be increased without deteriorating the

neutralization efficiency. This leads to the increase of beam injection power. In the deuterium experiment on LHD, two of the positive-ion based NBIs will increase their injection energy, i.e., one will increase from 40keV to 60keV and the other will increase from 40keV to 80keV, and both of their injection powers will increase from from 6MW to 9MW. The increase of Electron Cyclotron Heating (ECH) power is also planned by installing one more 154GHz gyrotron on LHD as an upgrade of heating devices.

The upgrade of the helical divertor is underway. With the upgrade, the structure of the divertor was changed from an open divertor structure to a closed divertor structure as shown in Fig. 4. Here, we have to note all of the cross sections shown in Fig. 4 are the cross sections of the LHD inboard-side Vacuum-Vessel (VV) at the mid plane as indicated by a dashed circle in Fig. 1. With the open divertor structure, the recycled neutrals easily return to the confinement region of plasmas as described in Fig.4 (a). Thus, the density control was difficult with this structure. With the upgrade of the divertor, the closed structure was introduced. With the closed structure, most of the recycled neutrals are compressed at the dome as illustrated in Fig. 4(b), and the recycling of the particles to plasmas is suppressed. Because the particle flux going to the divertor plates concentrate at the inboard side of the divertor at the inwardly shifted magnetic-axis (R_{ax}=3.6m, where R_{ax} denotes the position of the magnetic axis in major radius) configuration, which is the standard configuration on LHD during the deuterium experiment, as shown in Fig. 5(a), the upgrade to the closed structure was limited to the inboard side of the divertor (Fig. 5(b)).[15] Figure 5(c) shows the neutral pressure at the divertor region measured by experiments and calculated by EMC3-EIRENE numerical simulation code.[16-18] As shown in Fig. 5(c), the compression of neutral particles by the closed structure is demonstrated and the compression rate of 10-20 is realized both by experiments and by the simulation. To evacuate the compressed neutral particles, a new cryo-sorption pump for the closed divertor was developed. Figure 4(c) shows the cross

section of closed helical divertor with the cryo-sorption pump. Under the roof of the divertor dome, the two cryo-sorption panels with charcoal chips are installed. Charcoal chips are affixed on the panel as an absorption material using indium, and the panel is cooled by chilled helium gas.[19] Between the dome and the panel, liquid nitrogen cooled plates and louvers are placed to shield the panels from the radiation from their surrounding materials at the room temperature. The pumping ability of the panel was tested by installing the panel at a single toroidal section of the closed helical divertor in the 2015 Fiscal Year (FY). The pumping speed of about $20m^3/s$ at 10^{-2}Pa was confirmed by the test. The installation of these cryo-sorption panels proceeded in 2016 FY on four more toroidal sections, and the total pumping speed of up to $100m^3/s$ will be achieved with the panels. This will bring us low recycling condition, which is preferable to achieve high ion temperature plasmas,[20] on LHD plasmas.

As an upgrade of diagnostic systems, the neutron diagnostic is newly installed on LHD. Three sets of neutron flux monitors are installed on LHD. One is installed at the center top and the other two are installed at the outer mid plane of the LHD as shown in Fig. 1. Each sets consists of a ^{235}U fission chamber and either a ^{10}B proportional chamber (center) or a ^{3}He proportional chamber (outer midplane).[21] To evaluate the neutron profile of LHD plasmas during the deuterium experiments, an 11-channel neutron profile monitor[22] based on stilbene scintillators is also installed at the vertically elongated cross section of LHD as shown in Fig. 1.

The expected neutron emission rate in the LHD deuterium experiment is shown in Fig. 6. In evaluating the emission rate, the injection power of 14MW, which is the typical injection power in tNBI operation, is assumed for tNBI and that of 18MW is assumed for rNBI. Additional heating by ECH of 3MW is also assumed. In evaluating the emission rate, a model density profile of $(1-(r/a)^8)$ and a model temperature profile of $(1-(r/a)^2)^2$ are used. The

electron temperature and density is assumed to be equal to the ion temperature and density, respectively. Ions are assumed to consist of deuterium. The temperatures of the plasma are evaluated from the total absorbed heating power and the energy confinement time assuming the confinement improvement of two times larger than the International Stellarator Scaling 1995 (ISS95) law.[23] As shown in Fig. 6, the neutron emission rate of exceeding 10^{16}[n/s] can be expected. The majority of the neutrons are created by the reaction between the beam and bulk ions because the injection energy of tNBI is very high compared to the bulk-ion temperature and because the cross section for the D(d,n)^{3}He reaction strongly depends on the relative kinetic energy between the reactant ions.[24] This fact shows that the neutron diagnostic will be a good tool for evaluating the fast-ion confinement in the LHD deuterium experiment.

The NBIs are also the sources of neutrons when they are operated with the deuterium ion species. For example, neutrons can be produced at the neutral gas-cell and the residual ion dumps of the NBIs. The amount of neutrons produced at the LHD-NBIs was evaluated to be the order of 10^{13}n/s by following the manner shown by Kim.[25]

The amount of tritium produced by the deuterium experiment is evaluated from the neutron flux monitor because the cross section of D(d,p)T reaction is almost the same as that of the D(d,n)^{3}He reaction. Based on the agreement treaty with local government bodies for proceeding with the deuterium experiment on LHD, the tritium removal system[26] was installed at the end of the gas exhaust line of the LHD vacuum pumping systems as shown in Fig. 7. It must be noted that the tritium removal system discussed here removes all of the hydrogen isotopes from the exhaust gas as well as tritium. Hydrogen isotopes are removed from the gas using catalysts and are oxidized to water vapor. As tritium (hydrogen isotopes) removal systems, two types of water removal system are installed. One system is the molecular sieve type mainly used for exhausted gas from the vacuum pump during the

plasma experiment seasons and the other system is the polyimide membrane type for purged gas and ventilation during the maintenance seasons. The performance of the removal system was evaluated by experiments in 2015 FY. It was confirmed that the system fulfills its specification, which is to exceed the removal rate of 95% for hydrogen isotopes from the exhaust gas.

On the other hand, some of the instruments and facilities are either removed from the torus hall or moved from the hall to its basement or other places to avoid the influence by the neutrons and gamma-rays which will be produced from the deuterium experiment on LHD. In particular, most of the diagnostics using silicon semi-conductor detectors, such as Soft X-ray (SX) detectors,[27] hard X-ray spectrum analyzers,[28] and silicon diode based Fast Neutral Analyzers (FNA)[Ref.29], were removed from the LHD because the silicon semi-conductor detectors are known to be weak to irradiation by neutrons. As alternative choices for these diagnostics, installation of radiation hard detectors, such as SX detectors based on CsI scintillator[30] and FNAs based on artificial diamond detector,[31] and other detectors, are under investigation. To reduce the risk of the water-leakage during the initial phase of deuterium experiment, the ICRF antennas were also removed from the LHD-VV, tentatively.

4. Important Topics on the Deuterium Experiment

Evaluation of isotope effects in plasma confinement is one of the major tasks in the LHD deuterium experiments. The isotope effect in plasma confinement is widely observed in various tokamaks in the world.[32-37] It is often reported in the empirical scaling law based on the results of experiments that the energy confinement time (τ_E) is positively scaled with the mass number (A) of plasma ion species, e.g., $\tau_E \propto A^{0.5}$.[Ref.36] On the contrary, the gyro-Bohm scaling suggests that the confinement time would be scaled as $\tau_E \propto A^{-0.2}$.[Ref.35] The exponent of A in empirical scaling based on experiments varies with different discharge

scenarios and with different machines.[31-35, 37] Currently, no theory has succeeded in explaining the isotope effect on the confinement. In the stellarator, no clear dependence of the confinement time on mass is reported.[23] Thus, the investigation of the physical mechanism of the isotope effect is an important challenge for the deuterium experiments on LHD. As a preparation experiment for isotope effect studies on LHD, a set of discharges changing the bulk ion species from helium to hydrogen was performed using the NBI heated high-Ti plasmas on LHD.[Ref.38] In Fig. 8, the central electron and ion temperatures observed during the experiment are shown as a function of helium density fraction. In the discharges, electron density and temperature profiles were kept at almost the same values. The central electron and ion temperatures predicted by TASK3D simulation code[39] are also shown in Fig. 8. In evaluating the temperatures by the simulation, no dependence of thermal diffusivity on bulk ion species was assumed and only the difference of the slowing-down process of NB produced fast-ions due to the different bulk-ion contents was considered. As shown in the figure, the increase of ion temperature measured by the experiment was observed as the fraction of helium ion increases. On the contrary, no increase was observed for the predicted ion temperature by the TASK3D code with the variation of helium density fraction. The discrepancy between the simulation and experiment suggests the existence of ion thermal confinement improvement with the bulk ion species.

Demonstration of the confinement capability of Energetic Particles (EPs) in helical devices is another important topic of the LHD deuterium experiment. On LHD, confinement studies on EP were performed by using the Charge eXchange Neutral Particle Analyzer (CX-NPA) or Scintillator Lost Ion Probes (SLIP).[Ref.40, 41] The superiority of the inwardly shifted magnetic-axis configuration (R_{ax}=3.6m) was experimentally demonstrated by the ICRF tail measurement[41, 42] and by the decay time of energetic neutral measurement after the short pulse injection of rNB using CX-NPA.[Ref.44] The interaction between EP and EP-induced

instabilities were also intensively studied.[45-49] Figure 9 shows the parameter space for Alfven Eigenmode (AE) instability studies covered by various toroidal devices.[48] Because of the high energy tNBI and because of the wide operational ability of LHD in its magnetic field strength and in electron density, the parameter space covered by the LHD is the largest in the devices shown in the figure. This wide operational ability of LHD, especially in density, is a benefit of the stable currentless helical plasmas. This figure suggests that LHD is the one of the best toroidal devices for exploring the EP related physics in the world. During the non-deuterium experiment phase of LHD, the CX-NPA and SLIP are the main diagnostic tools for the EP studies on LHD. These diagnostics are very suitable for studying the details of EP behavior with EP-induced instabilities, i.e., the change of energy spectra and/or pitch angle distribution of EPs with these instabilities. On the other hand, it is very difficult to discuss the global EP confinement property with these diagnostics because their observed areas are very limited both in velocity phase space and in real space. In the deuterium experiment, neutron diagnostics will be powerful tools for evaluating the confinement properties of EPs because the neutron emission rate is dominated by the reaction between the energetic deuterium ions and bulk ions and because the EP information obtained by neutron diagnostic is integrated in velocity phase space of EPs. Thus, the neutron diagnostics are good tools for evaluating the global confinement properties of EPs. Recently, the experimental studies on EP confinement properties have received more interest than in the past because the ITG suppression by EP pressure gradient at low magnetic shear configuration was pointed out[50] and because of the EP profile stiffness by the multiple overlapping of small amplitude AEs.[Ref.51] Using the neutron profile monitor in the LHD deuterium experiment, we can explore the physics related to these phenomena and contribute to the understanding of EP confinement properties in the toroidal plasmas.

The PMI and hydrogen-isotope retention studies are the other important topics in the LHD deuterium experiment. As described in section 2, a new phenomenon in plasma-material interaction was recognized with the steady state operation on LHD. In the deuterium experiments, behaviors of fuel ions in material can be more clearly evaluated than in the hydrogen experiments because deuterium ion can be used as a tracer in materials. The retention studies of hydrogen-isotopes will also proceed in the deuterium experiments using tritium as a tracer. The amount of tritium produced in the deuterium plasmas can be evaluated from the neutron flux monitor as described in section 2, while the amount of tritium exhausted from the vacuum vessel can be monitored at the tritium removal system since all of the vacuum exhaust from peripheral devices, e.g. NBI, as well as LHD goes through the removal system. Thus, mass balance estimation on hydrogen isotopes can be performed quite accurately at the LHD deuterium experiment.

5. Summary

The aim of the Large Helical Device (LHD) project is to realize the high performance plasmas relevant to fusion plasma condition in Helical type magnetic configuration and to explore the related physics and engineering. The experiment was started in 1998. In the recent experiment on LHD, the high temperature operation region of LHD was intensively extended, e.g., ion temperature of 8.1keV at $1x10^{19}m^{-3}$ and electron temperature of 10 keV at $1.6\ x10^{19}m^{-3}$ were achieved, separately. To extend the performance of LHD, the upgrade of LHD, including the deuterium experiment, is planned. The deuterium experiment will be started in March 2017. The experiment will be conducted for nine years. The maximum annual neutron yield is $2.1x10^{19}$ neutrons for the first 6 years and is $3.2x10^{19}$ neutrons for the last three years. The upgrades of several devices are being conducted for improving the LHD performance. The helical divertors were modified to closed divertors with cryo-

sorption pumps in order to suppress the recycling from the divertor plates. The rNBIs, which are based on positive-ion sources, were also upgraded to increase their injection power from 6MW to 9MW for deuterium beam operation. As a preparation for the deuterium experiments, neutron diagnostics and tritium removal system are newly installed on LHD. The former will be used for annual neutron yield surveillance and will also become powerful tools for EP confinement studies. The latter was installed under the agreement with local government bodies and can be utilized to examine the mass balance of tritium in the vacuum vessel. Using these upgraded and/or newly installed devices, the performance of LHD plasmas will be improved and the LHD deuterium experiment will provide useful information to achieve the comprehensive understanding of toroidal plasmas as well as helical plasmas, i.e., the isotope effect, EP confinement properties, PMI and other important issues.

Acknowledgments

This work was supported by NIFS11ULGG801, NIFS10ULPP701, NIFS11ULPP801, NIFS11ULPP802, NIFS10ULRR010, NIFS10ULRR701, NIFS11ULRR801, NIFS11ULRR801, NIFS11ULRR802, NIFS11ULRR804, NIFS15ULAA708, and 10201042KEIN1601.

Plasma parameters	Achieved	Target
Ion temperature	8.1keV at 1×10^{19} m^{-3}	10keV at 2×10^{19} m^{-3}
Electron temperature	20keV at 2×10^{18} m^{-3} 10keV at 1.6×10^{19} m^{-3}	10keV at 2×10^{19} m^{-3}
Density	1.2×10^{21} m^{-3} at T_e of 0.25keV	4×10^{20} m^{-3} at T_e of 1.3keV
Beta	5.1% at 0.425T 4.1% at 1T	5% at 1-2T
Steady-state operation	54min. 28sec (0.5MW) (1keV, 4×10^{18} m^{-3}) 47min. 39sec. (1.2MW) (2keV, 1×10^{19} m^{-3})	1hour （3 MW）

Table I M. Osakabe

Experimental Campaign	First Campaign	Second to Sixth Campaign	Seventh to Ninth Campaign
Experiment	Preliminary (commissioning)	Exploration and characterization of deuterium plasmas	Integrated high-performance experiments
Maximum annual yield of Tritium	3.7×10^{10} [Bq] (integrated yield)		5.55×10^{10} [Bq] (integrated yield)
Maximum annual yield of neutron	2.1×10^{19} [n] (integrated yield)		3.2×10^{19} [n] (integrated yield)

TABLE II M. Osakabe

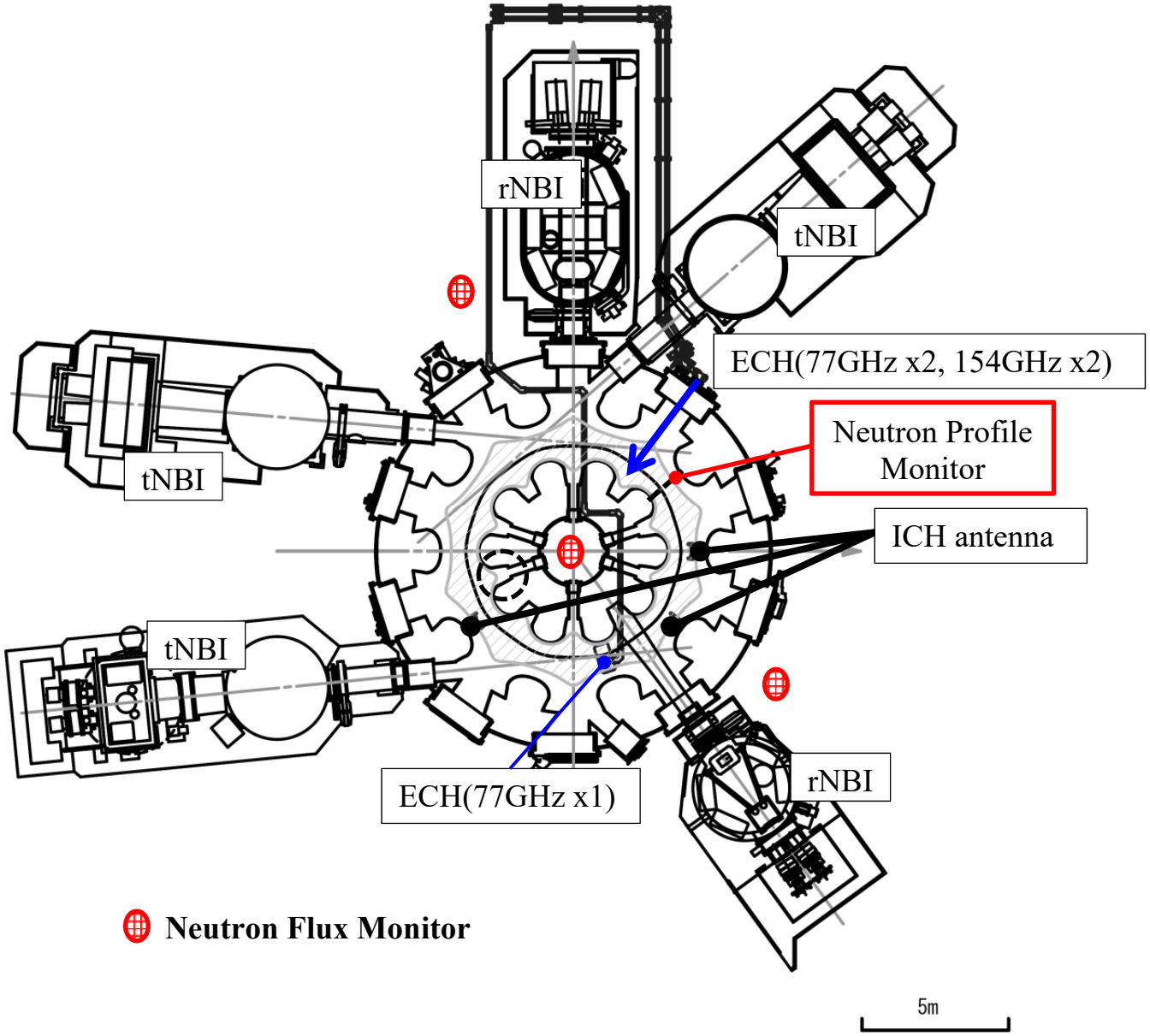

Fugure 1 *M. Osakabe*

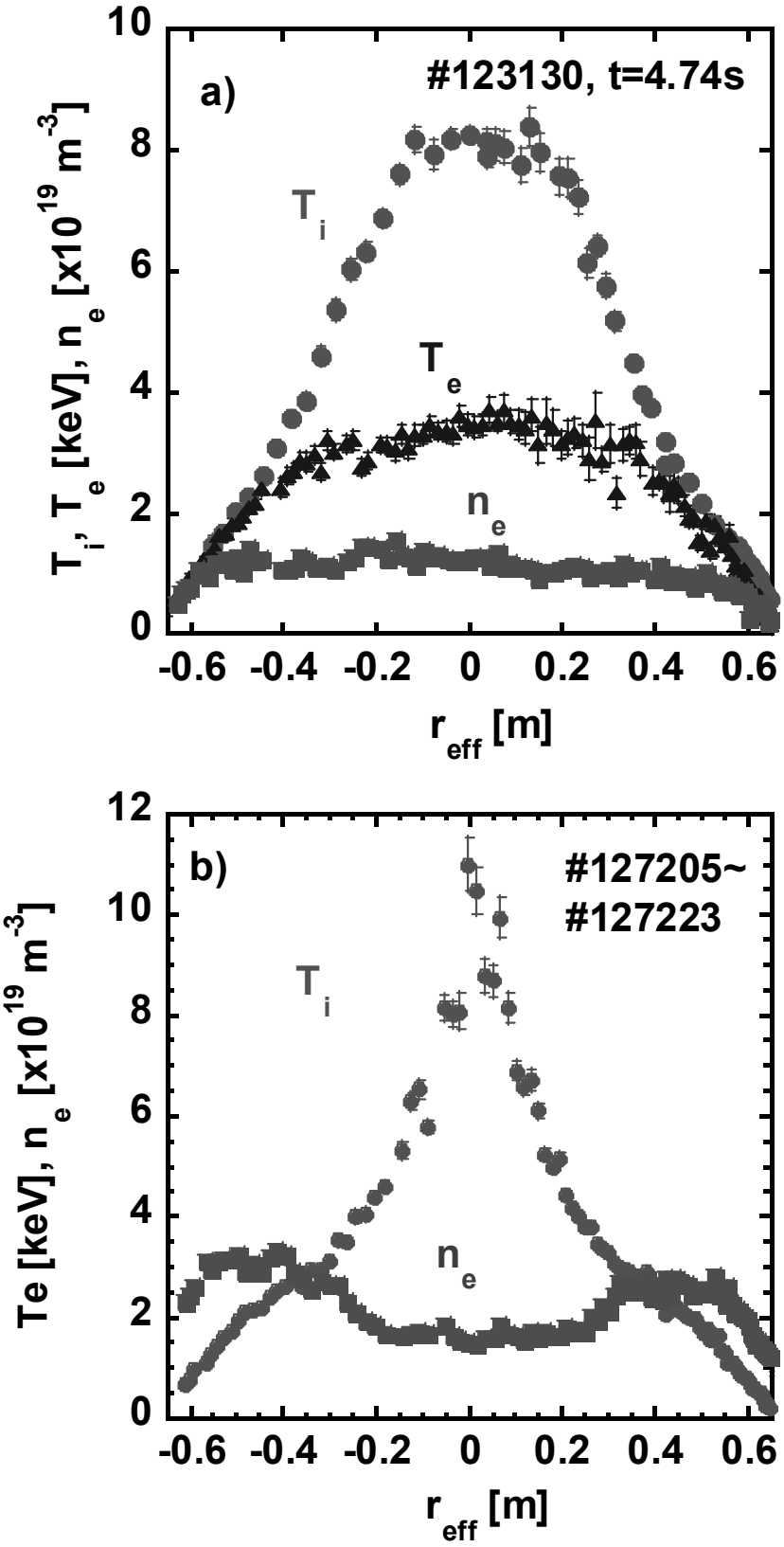

Figure 2 M. Osakabe

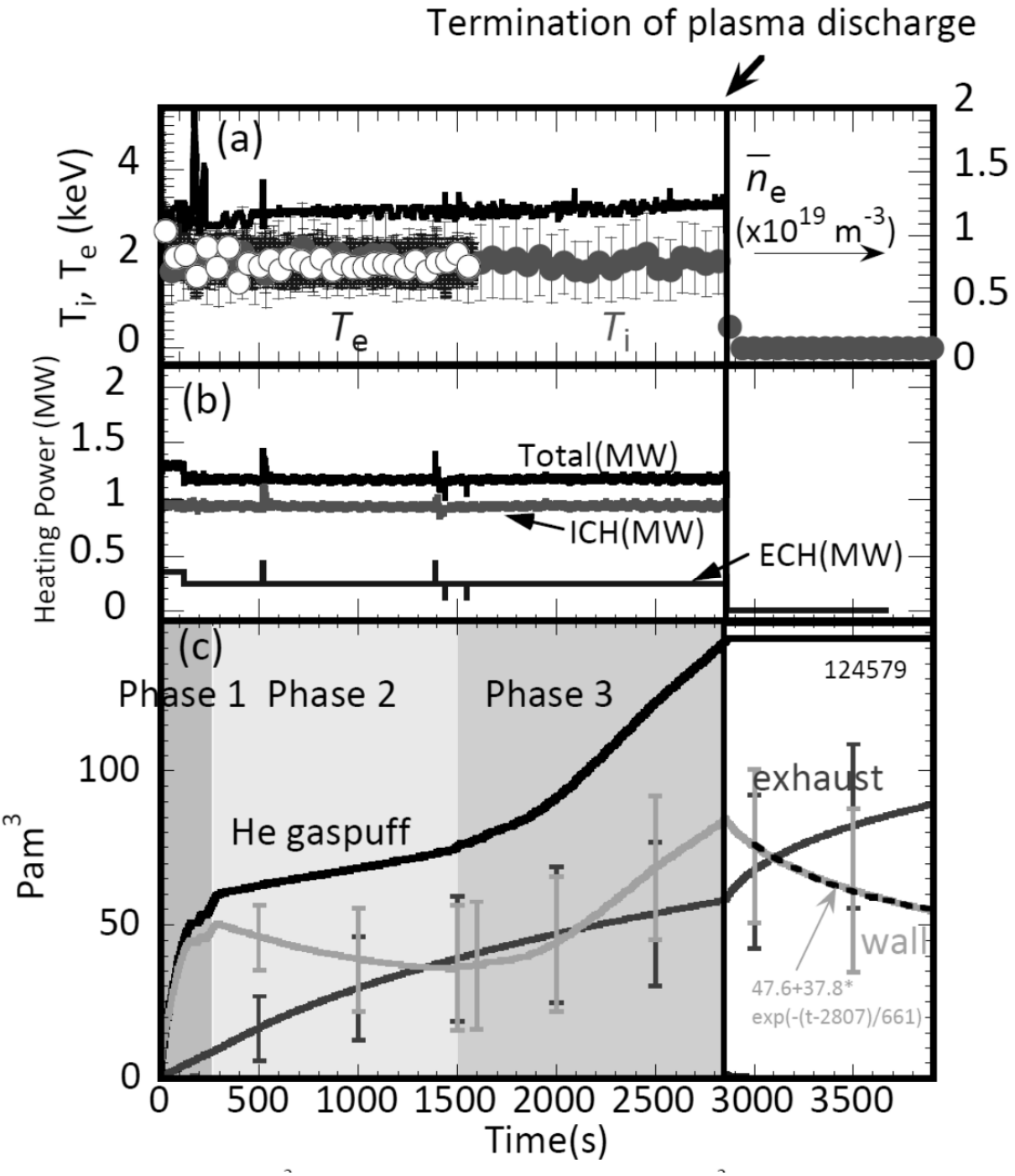

Figure 3 M. Osakabe

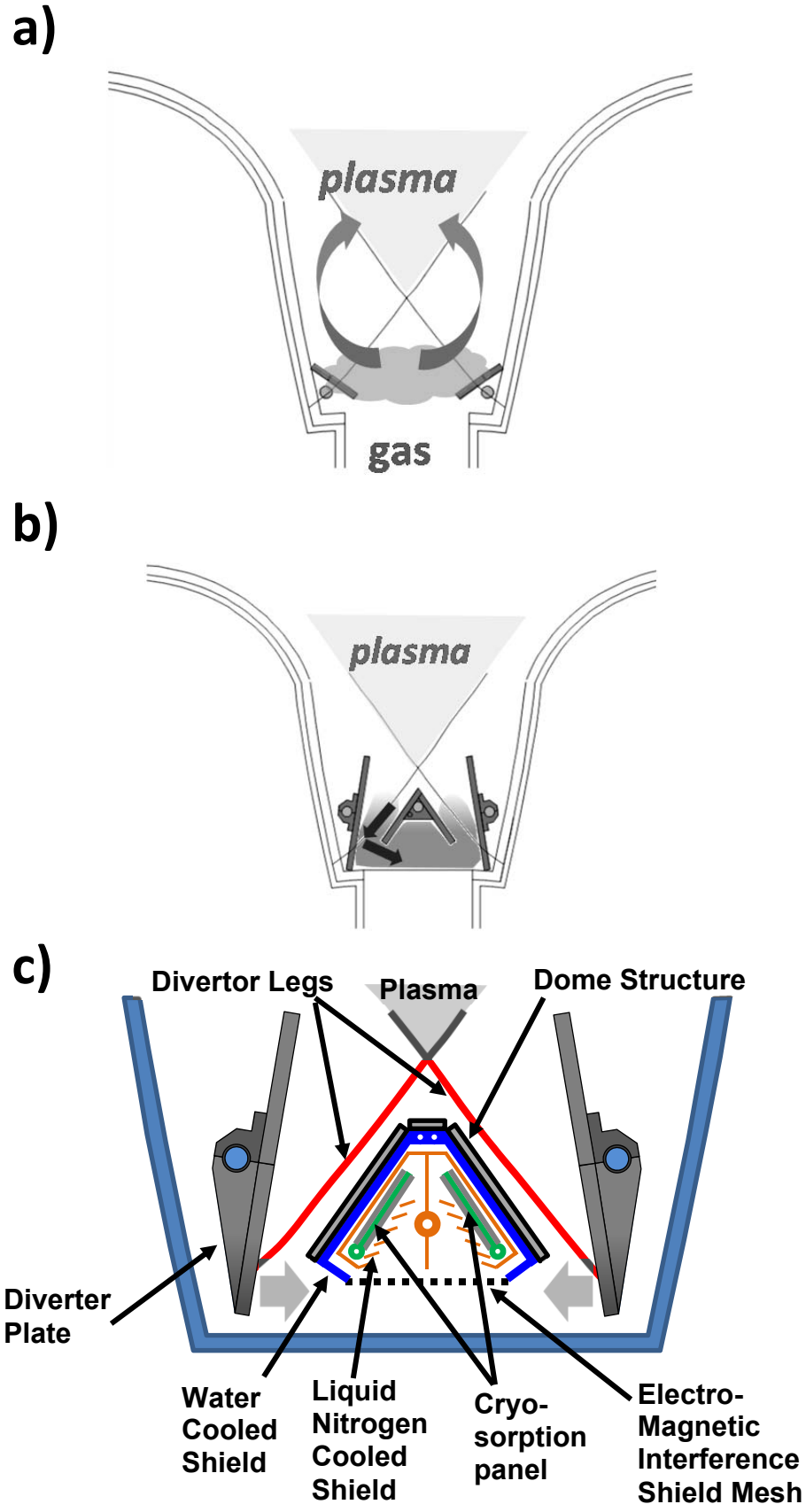

Figure 4 M. Osakabe

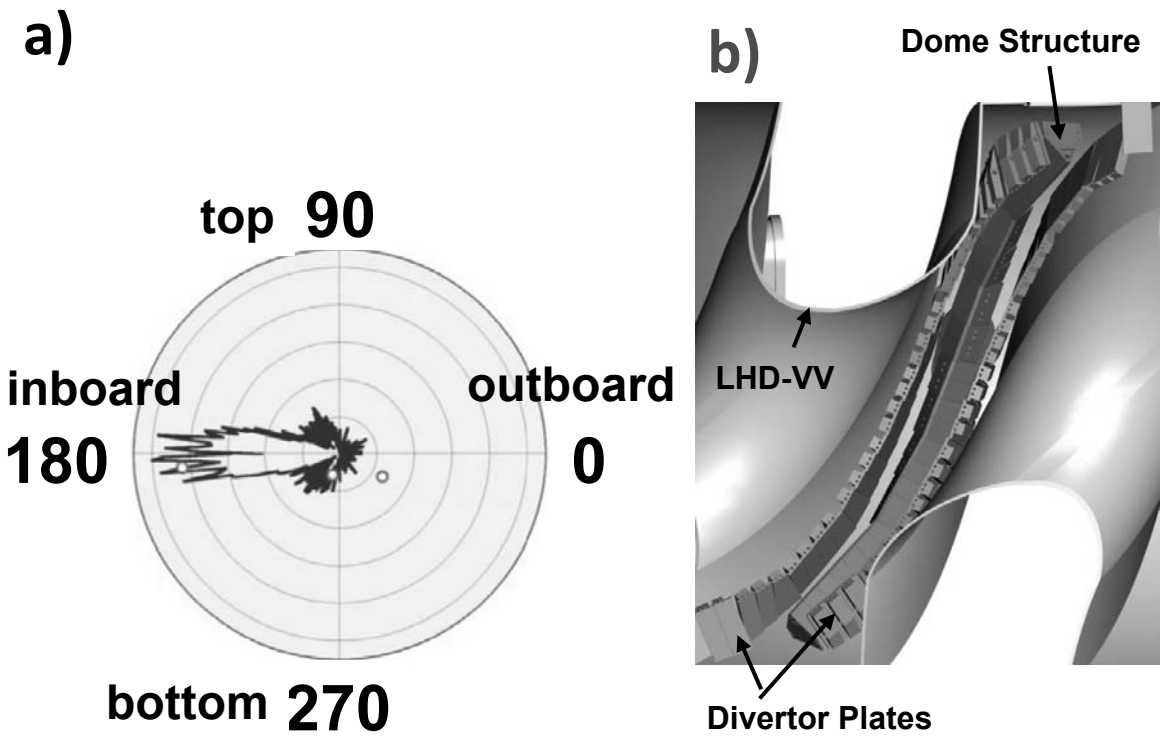

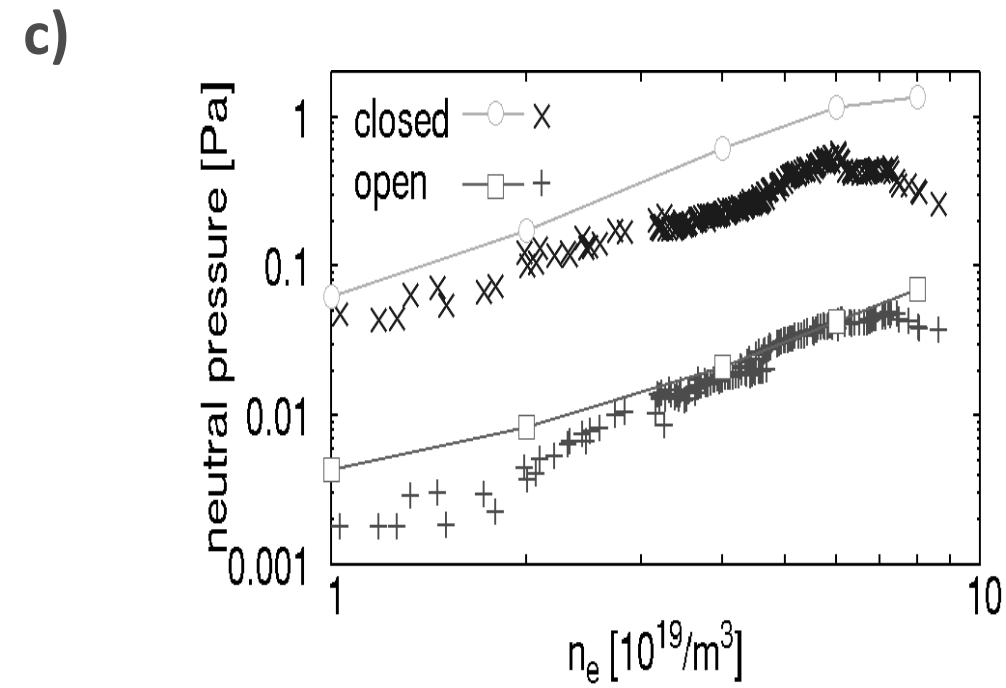

Figure 5 M. Osakabe

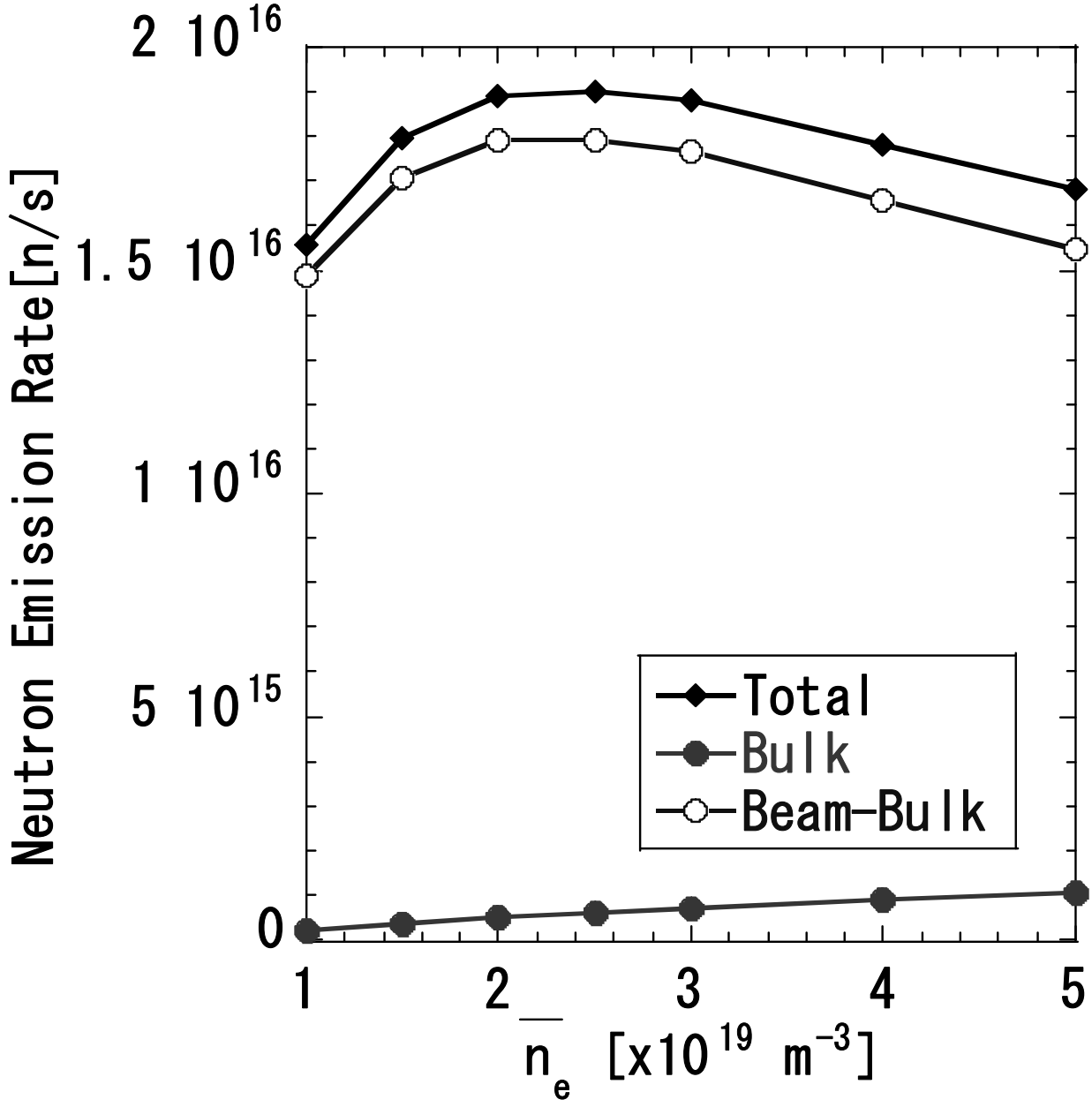

Figure 6 M. Osakabe

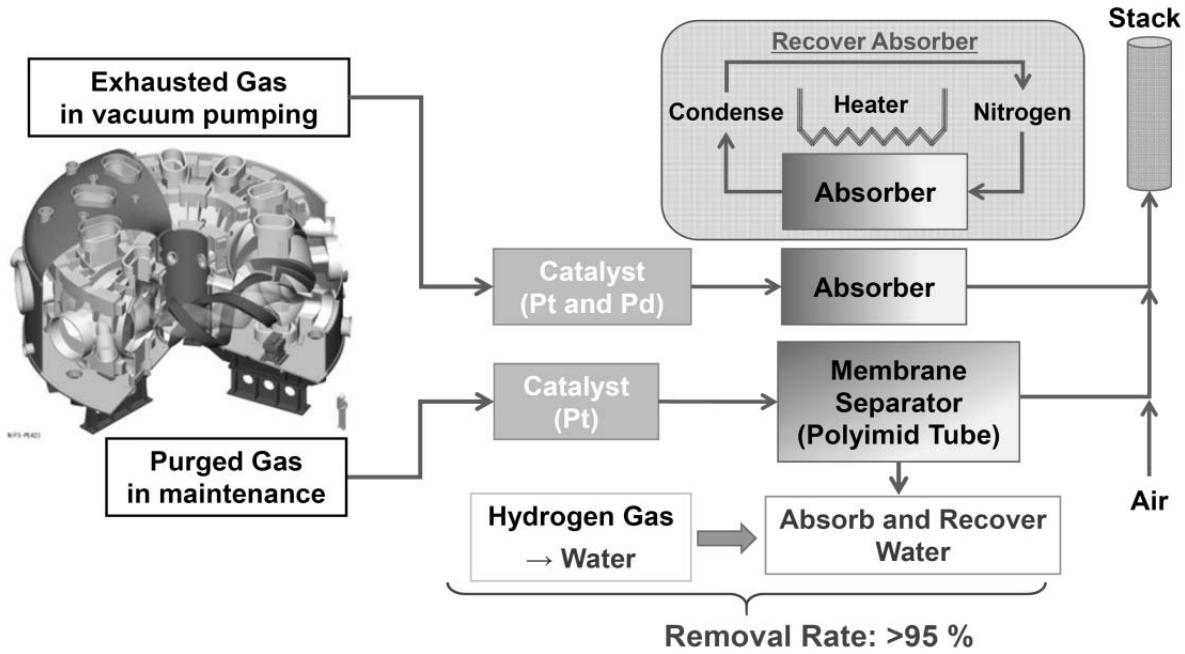

Figure 7 M. Osakabe

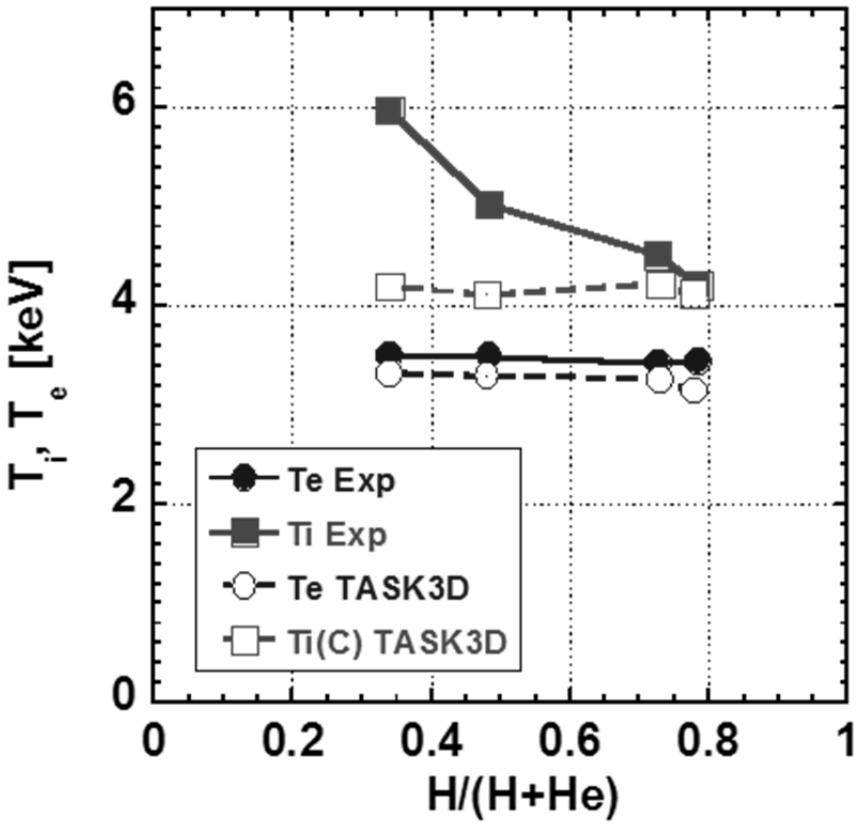

Figure 8 M. Osakabe

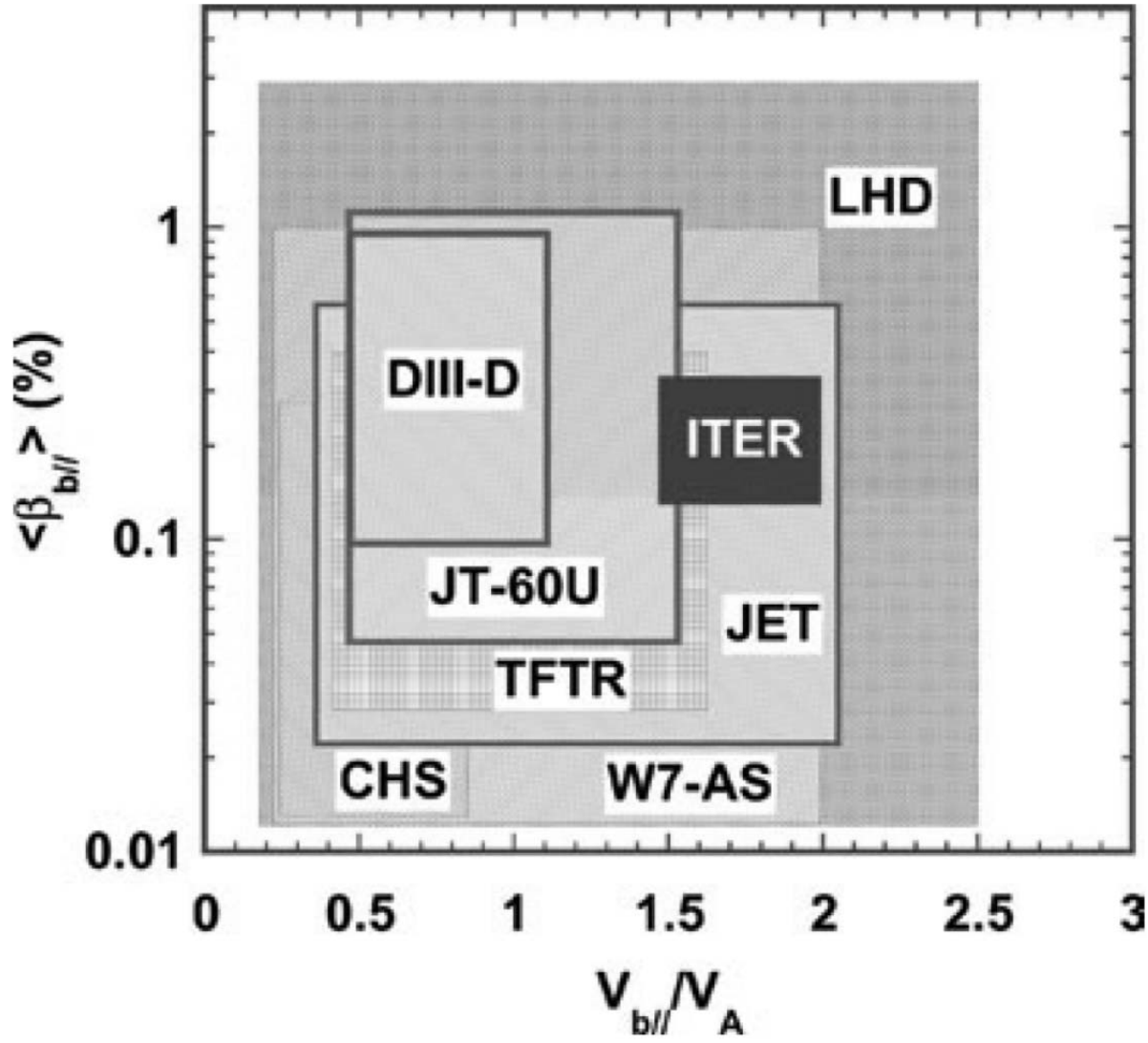

Figure 9 M. Osakabe

References

[1] A. Komori *et al.*, "Goal and Achievement of Large Helical Device Project" , Fusion Sci. Technol., **58**, 1 (2010)

[2] M. Osakabe *et al.*, "In-situ calibration of NBI injection power by the calorie meter at the counter wall", Rev. Sci. Instrum

[3] N. Noda *et al.*, "LHD Helical Divertor and Its Performance in the First Experiments", J. Plasma and Fusion Research SERIES, **3**, 180 (2000)

[4] Y. Takeiri *et al.*, " High Performance of Neutral Beam Injectors for Extension of LHD Operational Regime", Fusion Sci. Technol., **58**, 482 (2010)

[5] H. Takahashi *et al.*, "Extension of High T_e Regime with Upgraded Electron Cyclotron Resonance Heating System in the Large Helical Device", Phys. Plasmas, **21**, 061506 (2014)

[6] T. Mutoh *et al.*, "High Power Heating and Steady State Operation in the Large Helical Device", Fusion Sci. Technol., **68**, 216 (2015)

[7] K. Nagaoka *et al.*," Integrated Discharge Scenario for High-Temperature Helical Plasma in LHD", Nucl. Fusion, **55**, 113020 (2015)

[8] H. Takahashi *et al.*, "Effect of the RF Wall Conditioning on the High Performance Plasmas in the Large Helical Device", J. Nucl. Mater., **463**, 1100 (2015)

[9] M. Yoshinuma *et al.*, "Observation of an Impurity Hole in the Large Helical Device", Nucl. Fusion, **49**, 062002 (2009)

[10] M. Yoshinuma *et al.*, "Spontaneous Toroidal Flow and Impurity Hole in the High Ion Temperature Plasma on LHD", Fusion Sci. Technol., **58**, 103 (2010)

[11] T. Shimozuma *et al.*, "Improvement of Plasma Core Confinement via Electron-Root Realization by strongly focused ECRH in LHD: Core Electron-Root Confinement", Fusion Sci. Technol., **58**, 38 (2010)

[12] H.Takahashi *et al.*, “Extrension of high Te regime with upgraded electron cyclotron resonace heating system in the Large Helical Device”, Phys. Plasmas **21**, 061506 (2014)

[13] G. Motojima *et al.*, “Global Helium Particle Balance in LHD”, J. Nucl. Mater., **463**, 1080 (2015)

[14] K. H. Berkner *et al.*, “Intense, Mixed-Energy Hydrogen Beams for CTR Injection”, Nucl. Fusion, **15**, 249 (1975)

[15] T. Morisaki *et al.*, “Initial Experiments Towards Edge Plasma Control with a Closed Helical Divertor in LHD”, Nucl. Fusion, **53**, 063014 (2013)

[16] S. Masuzaki *et al.*, “Neutral Gas Compression in the Helical Divertor with a Baffle Structure in the LHD Heliotron”, Plasma Fusion Res., **6**, 1202007 (2011)

[17] G. Kawamura *et al.*, “First EMC3-EIRENE Simulations with Divertor Legs of LHD in Realistic Device Geometry”, Contrib. Plasma Phys., **54**, 437 (2014)

[18] D. Reiter *et al.*, “The EIRENE and B2-EIRENE Codes”, Fusion Sci. Technol., **47**, 2, 172 (2005)

[19] T. Murase *et al.*, “Development of New Concept In-Vessel Cryo-Sorption Pump for LHD Closed Helical Divertor”, Plasma Fusion Res., **11**, 1205030 (2016)

[20] H. Takahashi *et.al.*, “High Ion Temperature Plasmas using an ICRF Wall-Conditioning Technique in the Large Helical Device”, Plasma Fusion Res., **9**, 1402050 (2014)

[21] M. Isobe *et al.*, “Wide Dynamic Range Neutron Flux Monitor Having Fast Time Response for the Large Helical Device” , Rev. Sci. Instrum., **85**, 11E114 (2014)

[22] K. Ogawa *et al.*, “Progress in Development of the Neutron Profile Monitor for the Large Helical Device”, Rev. Sci. Instrum., **85**, 11E110 (2014)

[23] U. Stroth *et al.*, “Energy Confinement Scaling from the International Stellarator Database”, Nucl. Fusion, **36**, 1063 (1996)

[24] H. S. Bosch and G. M. Hale, “Improved Formulas for Fusion Cross-Sections and Thermal Reactivities”, Nucl. Fusion, **32**, 611 (1992)

[25] J. Kim, “D-D Neutron and X-ray Yields from High-Power Deuterium Beam Injectors”, Nucl. Technol., **44**, 315 (1979)

[26] M. Tanaka *et al.,* “Observations of the Gas Stream from the Large Helical Device for the Design of an Exhaust Detritiation System”, Plasma Fusion Res., **11**, 2405055 (2016)

[27] S.Ohdachi *et al.*, “Soft X-Ray Diagnostics on LHD”, Fusion Sci. Technol., **58**, 418 (2010)

[28] S.Muto, *et al.*, “First result from x-ray pulse height analyzer with radial scanning system for LHD”, Rev. Sci. Instrum. **72**, 1206 (2001)

[29] M. Osakabe, *et al.*” Development and energy calibration of Si-FNA for LHD fast ion measurement”, Rev. Sci. Instrum. **72**, 788(2001)

[30] T. Bando *et al.*, “Effects of Neutrons and γ-Rays on Scintillation Light in SX Diagnostics for LHD Deuterium Plasma Experiments”, Plasma Fusion Res., **10**, 1402090 (2015)

[31] T.Shimaoka *et al.*, “A diamond 14 MeV neutron energy spectrometer with high energy resolution”, Rev. Sci . Instrum. **87**, 023503(2016)

[32] M. Bessenrodt-Weberpals *et.al.*, “The Isotope Effect in ASDEX”, Nucl. Fusion, **33** (1993) 1205

[33] S. D. Scott *et al.* “Isotopic Scaling of Confinement in Deuterium-Tritium Plasmas”, Phys. Plasmas, **2**, 2299 (1995)

[34] R. J. Hawryluk *et al.*, “Results from Deuterium-Tritium Tokamak Confinement Experiments”, Rev. Mod. Phys., **70**, 537 (1998)

[35] J. Jacquinot *et al.*, “Deuterium-Tritium Operation in Magnetic Confinement Experiments: Results and Underlying Physics”, Plasma Phys. Controlled Fusion, **41**, A13

(1999)

[36] H. Urano *et al.*, "Energy Confinement of Hydrogen and Deuterium H-mode Plasmas in JT-60U", Nucl. Fusion, **52**(2012)114021

[37] P. N. Yushmanov *et al*., "Scaling for Tokamak Energy Confinement", Nucl. Fusion, **30**, 1999 (1990)

[38] K. Nagaoka *et al.*, "Comparison of Ion Internal Transport Barrier Formation between Hydrogen and Helium Dominated Plasmas", Plasma Fusion Res., **11**, 2402106 (2016)

[39] S. Murakami *et al.*, "Integrated Transport Simulations of High Ion Temperature Plasmas of LHD", Plasma Phys. Control. Fusion **57**, 054009 (2015)

[40] M. Osakabe *et al.*, "Fast-Ion Confinement Studies on LHD", Fusion Sci. Technol., **58**, 131 (2010)

[41] M. Isobe *et al.*, "Fast-Particle Diagnostics on LHD", Fusion Sci. Technol., **58**, 426 (2010)

[42] R. Kumazawa *et al.*, "Confinement Characteristics of High-Energy Ions Produced by ICRF Heating in the Large Helical Device", Plasma Phys. Control. Fusion, **45**, 1037 (2003)

[43] S. Murakami *et al.* "A Global Simulation Study of ICRF Heating in the LHD", Nucl. Fusion, **46**, S425 (2006)

[44] M. Osakabe *et al.*, "Evaluation of Fast-Ion Confinement Using a Radially Injected Neutral Beam in the LHD", Plasma Fusion Res., **5**, S2042 (2010)

[45] K. Ogawa *et al.*, "Magnetic configuration effects on TAE-induced losses and a comparison with the orbit-following model in the Large Helical Device", Nucl. Fusion, **52**, 094013 (2012)

[46] K. Ogawa *et al.,* "A study on the TAE-induced fast-ion loss process in LHD", Nucl. Fusion, **53**, 053012 (2013)

[47] M. Osakabe *et al.*, “Experimental observations of enhanced radial transport of energetic particles with Alfvén eigenmode on the LHD”, Nucl. Fusion, **46**, s911 (2006)

[48] K. Toi *et al.*, “MHD Modes Destabilized by Energetic Ions on LHD”, Fusion Sci. Technol., **58**, 186 (2010)

[49] K. Toi *et al.*, “Energetic ion driven Alfvén eigenmodes in Large Helical Device plasmas with three-dimensional magnetic structure and their impact on energetic ion transport”, Plasma Phys. Control. Fusion, **46**, S1 (2004)

[50] J. Citrin *et al.*, “Nonlinear Stabilization of Tokamak Microturbulence by Fast Ions”, Phys. Rev. Lett., **111**, 155001 (2013)

[51] C. S. Collins *et al.*, “Observation of Critical-Gradient Behavior in Alfvén-Eigenmode-Induced Fast-Ion Transport”, Phys. Rev. Lett., **116**, 095001 (2016)

TABLE I Target plasma parameters of LHD and its achieved value

TABLE II Schedule of deuterium experiments on LHD

Fig.1 A schematic view of LHD at the mid-plane and the alignment of heating sources. The location of neutron flux monitors and the neutron profile monitor are also shown.

Fig.2 (a) Typical ion temperature profile (red), electron temperature profile (blue) and electron density profile (green) of high ion temperature plasma on LHD, where ion temperature was measured by charge exchange spectroscopy, and electron temperature and density were measured by Thomson scattering diagnostic (From Ref.5). (b) Typical electron temperature (red) and density (green) profiles at the high electron temperature discharge. The profiles are obtained by accumulating the five identical shots (#127205, #127211, #127214, #127219 and #127223) at the timing of t=3.64s.

Fig.3 Waveforms of 47min. 39sec. steady state operation discharge. (a)The line averaged electron densities are shown by black lines, central electron temperatures are shown by blue open circles, and central ion temperatures are shown by red closed circles. (b)The input heating power by ECH and ICH are shown by blue lines and red lines, respectively. The black lines denote the sum of them. (c) The particle balance in the discharges are shown. The black lines show the fueling rate by the He gas puff, while the green lines are the particle exhaust rate by the external vacuum pumps. The orange lines are the subtraction of pumping rate from fueling rate.

Fig.4 Cross section of (a) open divertor structure, (b) closed divertor structure, and (c) closed divertor with cryo-sorption pump for the inboard side of one helical section at the mid plane.

Fig.5 (a) Poloidal distribution of particle flux to divertor plates at the inwardly shifted configuration. (From Ref.15) (b) The schematic view of the closed helical divertor which is installed at the inboard side of LHD vacuum vessel (From Ref.15). (c) Comparison of neutral pressure at the divertor region with the closed structure and the open structure. Neutral pressures measured by experiments are shown by crosses(x) for the closed structure and by plus(+) symbols for the open structure, while the open circles express the result of numerical simulation by EMC3-EIRENE for the closed structure and open squares express that for the open structure.

Fig.6 Maximum expected neutron emission rate at the LHD deuterium experiment.

Fig.7 Schematic drawing of the tritium (hydrogen isotopes) removal system from the exhaust gas of the vacuum pumps at LHD.

Fig.8 Variation of central electron temperature (blue closed circles with solid lines) and central ion temperature (red closed squares with solid lines) observed during H/(H+He) density ratio scan experiments. Central electron and ion temperature predicted by TASK3D code is also shown by open circles with dashed lines and by open squares with dashed lines, respectively (From Ref.38).

Fig.9 Parameter space scanned for Alfven Eigenmode (AE) studies in various toroidal devices. Horizontal axis denotes the velocity of energetic particles parallel to magnetic field which is normalized by Alfven velocity and vertical axis evaluates the components of energetic particle beta value parallel to the magnetic field line. (From Ref.49)